Chem. Res. Chin. Univ., 2016, 32(2), 311—317 doi: 10.1007/s40242-016-5272-x

Synthesis and Characterization of Novel UV-curable Fluorinated Polyurethane-acrylate Copolymer

WANG Honglei[1,2,3], LIU Weiqu[1,2*], TAN Jianquan[1,2,3] and XIAHOU Guolun[1,2,3]

1. Guangzhou Institute of Chemistry, Chinese Academy of Sciences, Guangzhou 510650, P. R. China;
2. Key Laboratory of Cellulose and Lignocellulosics Chemistry, Chinese Academy of Sciences, Guangzhou 510650, P. R. China;
3. University of Chinese Academy of Sciences, Beijing 100049, P. R. China

Abstract A series of UV-curable fluorinated polyurethane-acrylate(PUA) has been developed by incorporating octafluoropentyl alcohol into the segment of UV-curable polyurethane-acrylate to improve the thermal property and surface property of the copolymer material. The structures of the synthesized polymers were characterized by Fourier transform infrared(FTIR) spectrometry. In order to find out the effect of incorporated fluorine on the UV-cured films, the properties of the UV-cured films were tested through contact angle, water absorption, and thermogravimetric analysis (TGA). The fractured-surface morphologies of the UV-cured coatings were investigated by scanning electron microscopy(SEM). With increasing the content of fluorine segments, the contact angle of the UV-cured films increased and the water absorption decreased, suggesting the fluorine segments migrated and formed a fluorine-covered surface to avoid water penetration. The observation of the fractured-surface morphology through SEM test showed that the fluorinated UV-cured films gained rough fractured-surface compared with the pure UV-cured polyacrylate film, demonstrating the migrating of the fluorine segments. The TGA curves show that the fluorinated UV-cured films gained higher thermal degradation temperature than the virgin UV-cured polyacrylate film. And as increasing the fluorine content, the thermal degradation temperature increased. These phenomena could be reasonably explained by the enrichment of fluorine-contained segment on the surface of the film and the high thermal property due to fluorine atom.

Keywords Fluorinated polyurethane; Functional acrylate oligomer; UV-cured film; Hydrophobic surface

1 Introduction

UV-curing has become a widely used technology in polymer science for its advantages[1—4], such as reduced solvent emission, rapid curing speed, and the ability to coat heat-sensitive devices under moderate curing conditions[5—7]. Polyurethane has been widely used for its good toughness, flexibility, and elongation[8—12], however, it couldn't cure under UV light in its original state. Various properties and enhanced performance could be obtained for polyurethane-acrylate(PUA). UV-active PUA oligomer cured by UV-light could form interpenetrating networks, which may combine the beneficial properties of polyurethane(PU) and polyacrylate(PA) components. Through choosing proper raw materials, a certain UV-curable PUA structure could be formed easily. UV-curable PUA materials can be satisfactorily applied in coatings, biologic materials, electronic materials, textiles, leather and printing inks[13]. However, simple PUA films have been found not to be good enough to resist water on account of the hydrophilic surface of the films[14].

Fluorinated polymers have been diffusely applied in hydrophobic coating and used as medical devices because of their excellent properties of environmental stability, water and oil repellency, thermal stability and chemical resistance and low interfacial free energy[15—18]. Consequently, fluorine-contained polymers have been widely applied in many upscale technologies, including automotive and aerospace industries, and used as optical and microelectronic instruments[19—22]. Recently, researchers have done extensive work on fluorinated polyacrylate and fluorinated polyurethane for their advanced all-around properties. Lu *et al*.[23] did researches on a series of core-shell acrylic copolymer latexes containing fluorine enriched in the shell through emulsion polymerization. The surface segregation of poly(*n*-alkyl methacrylate) end-capped with varying numbers of units of 2-perfluorooctylethyl methacrylate was investigated by Wang's group[24]. And they also conducted an investigation in a kind of fluorinated copolymers of poly(methyl methacrylate)-b-poly(butyl methacrylate) or poly(*n*-cotadecyl methacrylate) end-capped with 2-perfluorooctylethyl methacrylate[19]. Tan *et al*.[25] synthesized a series of fluorinated polyurethanes with fluorinated side chain attached on hard segment. Honeychuck *et al*.[26] used a series of ethylene-fluoroakyl-ethylene diols and hexamethylene diisocyanate(HDI) to prepare fluorinated polyurethanes. Mostly,

*Corresponding author. E-mail: liuwq@gic.ac.cn

Received July 14, 2015; accepted December 29, 2015.

Supported by the the Science and Technology Program of Guangzhou City, China(No.2014J4100215), the Natural Science Foundation of Guangdong Province, China(No.S2013010012106) and the Project of the Key Laboratory of Cellulose and Lignocellulosics, Guangzhou Institute of Chemistry, Chinese Academy of Sciences.

researches were focused on introducing fluorinated acrylate into polyacrylate or incorporating fluorocarbon chains into polyurethane to obtain fluorinated polyacrylate and fluorinated polyurethane, respectively. However, in order to investigate the advanced UV-curable PUA materials, there is an ever increasing demand for fluorine modified PUA with improved properties.

In this work, a novel fluorinated polyurethane(FPU) reactive oligomer was prepared based on tolylene diisocyanate (TDI), polyether glycol(M_w=2000), polyether polyol(N220), and octafluoropentyl alcohol. Octafluoropentyl alcohol was incorporated into the segment of polyurethane to improve the thermal property and surface property. Double bonds were introduced into reactive polyacrylate oligomer to obtain photopolymerization functionality. The newly synthesized FPU was introduced at different ratios into polyacrylate coating mixture. A series of novel fluorinated PUA(FPUAs) used for UV-curing systems was synthesized and characterized with Fourier transform infrared(FTIR) spectrometry. Furthermore, the surface hydrophobic and thermal properties of the UV-cured coatings made from the obtained polymers were investigated by gel content test, flexibility test, pencil hardness test, contact angle(CA) analysis, and thermogravimetric analysis(TGA). The fractured-surface morphologies of the UV-cured coatings were investigated by scanning electron microscopy(SEM).

2 Experimental

2.1 Materials

Dibutyltin dilaurate(DBTDL) was purchased from Nantong Hongding International Chemical Industry Co., Ltd., China. Linear polyether polyol(N220, M_w=2000) was provided by Guangzhou Longhui Chemical Industry Co., Ltd., China and vacuum dried at 120 °C for 4 h before use. Octafluoropentyl alcohol was obtained from Beijing JHYB Pharmaceutical Technology Co., Ltd., China. 2,2-Azobisisobutyronitrile (AIBN) and 2,6-di-tert-butyl-4-methylphenol(BHT) were purchased from Tianjin Kermel Chemical Industry Co., Ltd., China. Glycidyl methacrylate(GMA) and isobutyl methacrylate(IBMA) were purchased from Xinghuo Chemical Co. of China. Tetrabutylammonium bromide(TBAB) was supplied by Aldrich Chemical Co. and 2-hydroxy-2-methylpropiophenone (Irgacure 1173) was obtained from Ciba Chemicals. Methacrylic acid (MA) and 2-hydroxyethyl methacrylate(HEMA) were purchased from Shanghai Hechuang Chemical Co., Ltd., China. 2,4-Tolylene diisocyanate(TDI) was manufactured by Cangzhou Dahua Group Co., Ltd., China. Microscope slides were provided by Shanghai Jingke Industrial Ltd., China.

2.2 Syntheses of Polyacrylate and FPUA

Polyacrylate was prepared from GMA, HEMA and IBMA at a mass ratio of 1:1:8 in the presence of 4%(mass fraciton) AIBN as initiator and butanone as solvent at a temperature of 80 °C. The reaction was carried out in a three-neck reaction kettle equipped with a magnetic stirrer, nitrogen inlet, water condenser and thermometer. The reaction was carried out for 8 h to obtain desired product. Subsequently, butanone was removed by reduced pressure distillation. The retained desired product was labeled as GHI and was transfered into another three-neck kettle. Afterwards, a certain amount of MA was added in the kettle in the presence of TBAB. Toluene was added to it as solvent. The reaction was carried out at 102 °C to reach 99.5% of the conversion determined by standard acid value. After remained toluene and unreacted MA were discarded by reduced pressure distillation, the product was obtained and labeled as PA. The general procedure is shown in Scheme 1.

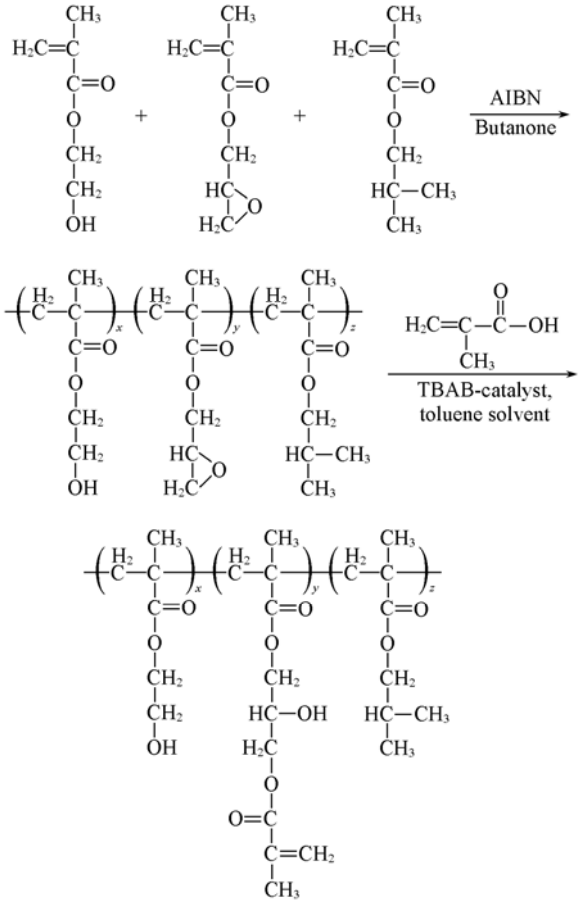

Scheme 1 Synthesis route of UV-cured PA

Polyether polyol(N220) and TDI at a mass ratio of 100:14 were placed into a three-necked reaction kettle equipped with a mechanical stirring rod, a thermometer, and a nitrogen inlet. The mixture was heated to 80 °C under nitrogen for 4 h. Subsequently, a certain amount of octafluoropentyl was dropped into the reactor and stirred for another 3 h. FPU product was not obtained until the —NCO content reached the theoretical value determined by dibutylamine titration(Scheme 2). Then a certain quantity of PA dissolved in dimethylbenzene with a mass ratio of 1:2 was added dropwisely to it at 80 °C for 30 min upon stirring. DBTDL(0.2%, mass fraciton) was added to it as catalyst. The reaction was then carried at 80 °C. Product was obtained and labeled as FPUA when —NCO peak at 2270 cm^{-1} disappeared totally in the FTIR spectra of the samples taken from the reaction medium every 0.5 h. The synthesis route of the whole reaction process is depicted in Scheme 3.

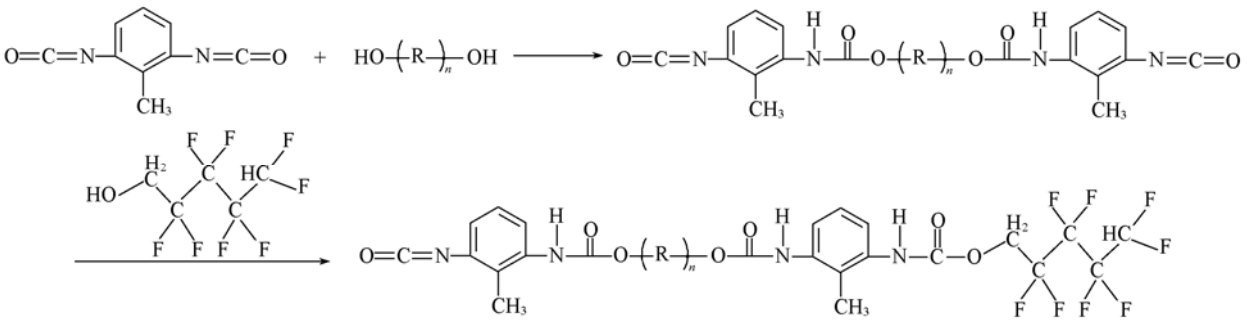

Scheme 2 Synthetic route of FPU

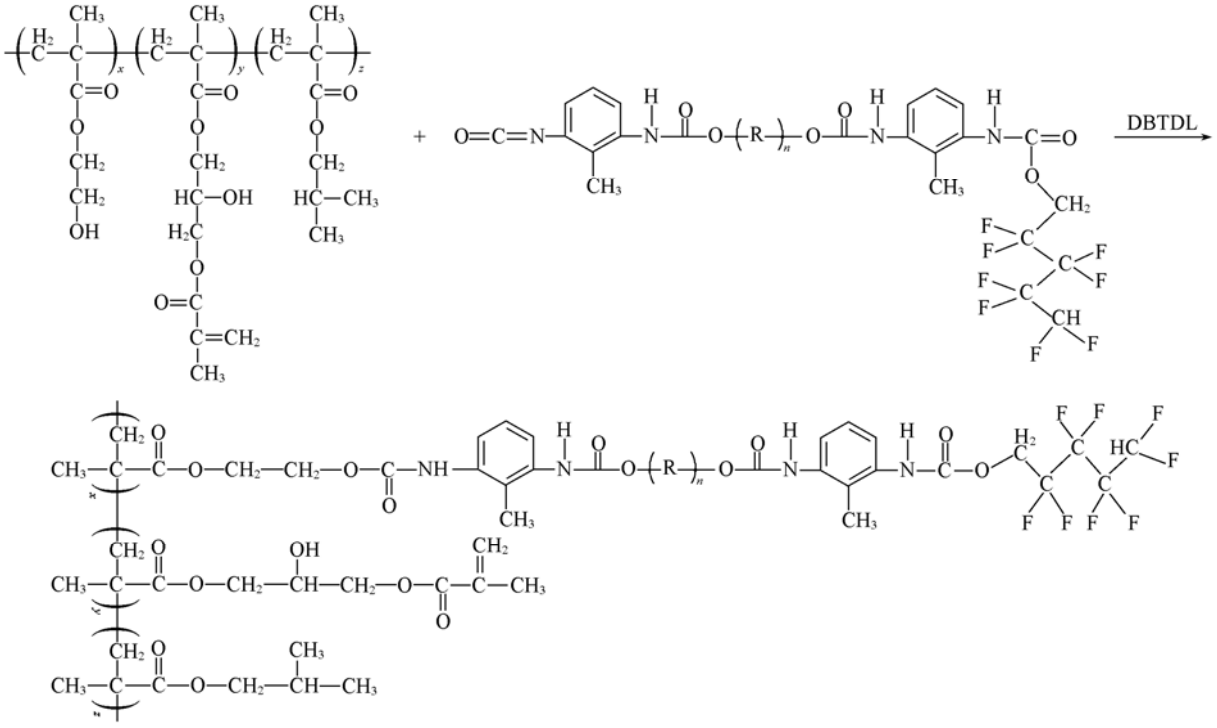

Scheme 3 Synthetic route of FPUA

The ratios of FPU and PA can be seen in Table 1.

Table 1 Ratios of FPU to PA and variations of FPUAs

Sample	*m*(FPU)/g	*m*(PA)/g	*w*(Fluorine)(%)
FPUA1	11.88	88.12	1
FPUA2	23.76	76.24	2
FPUA3	35.64	64.36	3
FPUA4	47.52	52.48	4
FPUA5	59.41	40.59	5
FPUA6	71.29	28.71	6

2.3 Preparation of FPUA UV-curable Films

The photoinitiator Irgacure 1173 and the reactive oligomer FPUA were mixed together. Photoinitiator at 5%[*m*(Irgacure 1173):*m*(triethanolamine)=2:3] was added to the mixture upon stirring for 10 min. Triethanolamine was used to avoid the oxygen inhibition during the UV-curing process. The coating mixtures were cast onto microscope slides at room temperature by a wire-gauged applicator. And they were put in an oven at 80 °C for 1 h and then an vacuum oven at 70 °C for 0.5 h to remove the dimethylbenzene solvent to obtain a homogeneous thickened coating layer. The applied coatings were situated in a place 20 cm below a UV processor with a high-pressure mercury lamp(500 W, λ_{max}=365 nm) and were irradiated for 30 s in air atmosphere. The thickness of the final coated film is about 100 μm.

2.4 Characterization

The FTIR spectra were recorded with a TENSOR27 spectrometer(Bruker, Germany) over a range of 400—4000 cm^{-1}.

The gel content method was performed on the cured films by measuring the mass loss after a 48-h extraction at 80 °C, according to the standard test method ASTM D2665-84[27]. It was calculated as:

$$\text{Gel content}(\%)=m_t/m_0\times100\% \quad (1)$$

where m_0 is the initial mass of the film, and m_t is the final mass after extraction.

Flexibility of the UV-cured films was measured according to standard test method(ASTM D522) for elongation of attached coatings with conical mandrel apparatus(QTY-32, Shanghai Junda Co., China)[28]. Pencil hardness test was conducted on UV-cured films according to the Stander test method ASTM D2263[29].

The contact angle measurement was done *via* an optical contact angle meter(Shanghai Zhongchen, China) at room temperature(25 °C) for water and ethylene glycol as pendant drops. Each sample was tested more than 5 times at different locations and averaged readings were recorded to obtain a reliable value. The surface free energy was calculated by means of geometric-mean equation which was described by Owens and Wendt[30]. According to Owens and Wendt, the surface energy of a given solid can be determined with the help of an equation applied to two liquids[30].

$$(1+\cos\theta)\gamma_l=2(\gamma_s^d\gamma_l^d)^{1/2}+2(\gamma_s^{nd}\gamma_l^{nd})^{1/2} \quad (2)$$

where γ_s and γ_l are the surface free energies of the solid and pure liquid, respectively. The superscripts 'd' and 'nd' represent the dispersive and non-dispersive contributions to the total surface energy, respectively, with water(γ_l=72.8 mJ/m^2, γ_l^d=21.8 mJ/m^2, γ_l^{nd}=51 mJ/m^2), and ethylene glycol(γ_l=48 mJ/m^2, γ_l^d=29 mJ/m^2, γ_l^{nd}=19 mJ/m^2). According to Pinnau and Freeman[31], the contact angle, θ, in Eq.(2) was obtained from the following equation:

$$\theta=\cos^{-1}[(\cos\theta_a+\cos\theta_r)/2] \quad (3)$$

where θ_a and θ_r are the advancing and receding contact angles, respectively. Water absorption(P) measurement of UV-cured samples was carried out in distilled water at 25 °C according to ASTM D570. The fresh films were removed from the microscope slides carefully and were dried for 24 h in a vacuum oven at 60 °C. Weighed samples were kept in water for at least 48 h until equilibrium was attained. At set time intervals, the samples were removed, blotted with absorbent paper and accurately weighed. The water absorption value of UV-cured samples was calculated from the ratio of the mass of absorbed water to that of the dry polymer[32],

$$P(\%)=[(m_s-m_d)/m_d]\times100\% \quad (4)$$

where m_s is the mass of the swollen sample and m_d is the mass of the sample dried under vacuum.

The refraction index of the coating was determined *via* an Abbe refractometer(WAY-2W, Shanghai Electronics Physical Optics Instrument Co., Ltd., China) at 25 °C.

Cross-section morphologies of the fracture cured coating films were studied by environmental scanning electron microscopy(SEM, Hitachi S-4800 FESEM). For SEM inspection, samples were fixed to aluminum stubs with conductive tape prior to coating a layer of gold with *ca*. 20 nm in an Ernest Fullam sputter coater.

The thermal stability of cured polymeric materials was determined on a thermogravimetric analyzer(TGA, TG209F3, NETZSCH, Germany). The thermogravimetric analysis of selected coatings was carried out at a heating rate of 20 °C/min under nitrogen atmosphere(flow rate is 30 mL/min) in a temperature range of 40—600 °C.

3 Results and Discussion

3.1 Synthesis and Characterization of FPUA

Six UV-curable fluorinated samples FPUA1, FPUA2, FPUA3, FPUA4, FPUA5 and FPUA6 were firstly synthesized in this work. The general synthetic process of the copolymer in the coating mixtures is mentioned in Scheme 3. FTIR spectra were recorded to characterize the structures of the products. The FTIR spectra of PA, PU and FPU samples are shown in Fig.1. The six UV-cured coating mixtures of FPUA are similar to each other and FPUA3 is shown in Fig.1. In the spectra, curve *a* of PA sample shows characteristic bonds of hydroxyl groups at 3525 cm^{-1}. The peak at 1640 cm^{-1} is attributed to C═C stretching vibration, indicating that the carboxyl of methacrylic acid reacted with epoxide group and C═C group was incorporated into the polyacrylate oligomer. FTIR analyses of PU and FPU are shown in curve *b* and curve *c*. In comparison of curve *b* with curve *c*, the weaker absorption bands at 2270 cm^{-1}(—NCO) and the stronger absorption bands at 3300 cm^{-1}(stretching vibration of the urethane ═NH bond) could be ascribed to the reaction between PU and octafluoropentyl alcohol. Curve *d* exhibites the stretching vibrations of —CF_2 and —CF_3 groups at about 1367 and 1232 cm^{-1} and also double bond groups at 1640 cm^{-1}. In the spectra, characteristic peaks of C═O(1700—1730 cm^{-1}) and C—H aliphatic stretching bands(2945, 2858 cm^{-1}) are also observed.

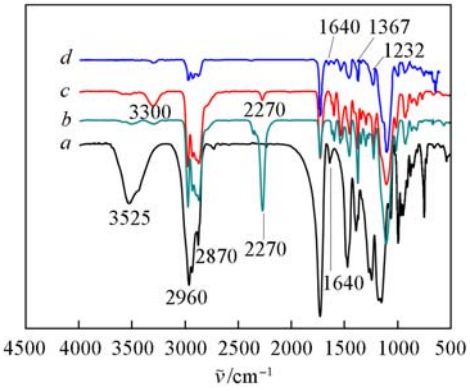

Fig.1 FTIR spectra of PA(*a*), PU(*b*), FPU(*c*) and FPUA3(*d*)

3.2 Gel Content, Flexibility and Hardness Characterization of the UV-cured Coatings

For the purpose of assessing the amount of insoluble part in cured films and the mechanical properties of the cured coatings, the gel content, flexibility, and pencil hardness of them were determined. In Table 2, the measured values are summarized. The gel content values of all the films are high enough to indicate the nearly complete cross-linked network of pure PA and composite FPUAs. In terms of flexibility, all the composite FPUA samples passed the tests of 8, 6 and 5 mm diameter, while the pure PA sample failed all the tests of 8, 6

Table 2 Gel content, flexibility and hardness of the UV-cured coatings

Sample	Gel content(%)	Flexibility			Pencil hardness
		8 mm	6 mm	5 mm	
Pure PA	96	Fail	Fail	Fail	3H
FPUA1	98	Pass	Pass	Pass	2H
FPUA2	97	Pass	Pass	Pass	2H
FPUA3	98	Pass	Pass	Pass	H
FPUA4	97	Pass	Pass	Pass	H
FPUA5	97	Pass	Pass	Pass	HB
FPUA6	97	Pass	Pass	Pass	HB

and 5 mm diameter. The hardness value of the samples changes from 3H to HB with increasing the amount of fluorine-contained PU. The flexibility and hardness tests suggested that the introduction of organic-fluorine segment enhanced the flexibility of the UV-cured coatings which would make it suitable for soft substrate such as the leather and textiles.

3.3 Water Absorption

The water absorption behavior of the UV-cured coatings is shown in Fig.2. The degree of water absorption decreased with the increase of fluorine percent. There was a sharp decline of the FPUA1 water absorption compared with virgin PA when fluorine content increased from 0 to 1%. However, when fluorine content exceeded 3%, the water absorption of the films changed slightly. The lower degree of water absorption of FPUA films, as compared to that of PA, shows that fluorine-contained polymer improved the water resistance of the UV-cured films due to the excellent hydrophobicity of fluorine.

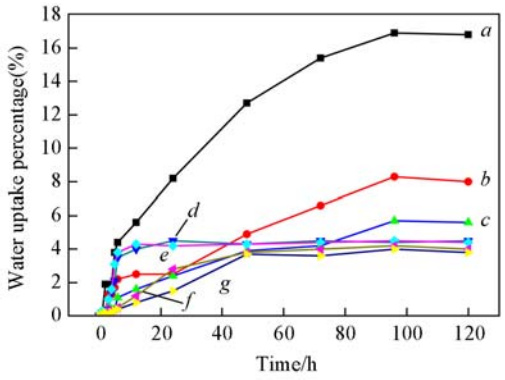

Fig.2 Water uptake percentage of UV-cured FPUAs *versus* time compared with that of PA

a. PA; *b*. FPUA1; *c*. FPUA2; *d*. FPUA3; *e*. FPUA4; *f*. FPUA5; *g*. FPUA6.

3.4 Surface and Optics Characterization of the Cured Coatings

In order to determine the effect of organic fluorine on the surface properties of the UV-cured FPUA films, contact angle was tested[33—35]. The surface free energies of the UV-cured samples, as characterized by static water contact angle, are summarized in Table 3. It can be seen that contact angles of both water and ethylene for pure PA film are much lower than those of any FPUA cured film. With the increasing of fluorine content, the contact angle on FPUA cured film surfaces showed a gradually increasing trend. It was found that based on the increase of fluorine concentration, FPUA tended to be more hydrophobic compared with the virgin PA. This was an expected behavior, assuming that fluorine groups could easily move towards the air-polymer interface thus making the surface more hydrophobic[36]. Thereby, the presence of fluorine could lead to a great decrease in the surface free energy, and among these composite films, FPUA6 presented a low surface free energy value down to 16.58 mN/m. Surfaces from the coating mixture of PA/ FPU at a ratio of 1:0.01 still show hydrophobicity although the fluorine content is low. The results shown in Table 3 indicate that fluorine-contained PU contributes to the surface hydrophobicity.

Table 3 Contact angles and surface free energies of UV-cured coatings

Sample	γ_s^*/(mN·m^{-1})	Contact angle, θ/(°)	
		Deionized water	Ethylene glycol
PA	26.15	85.5	62.5
FPUA1	19.15	94.5	75.5
FPUA2	19.31	96	76
FPUA3	19.42	101	79
FPUA4	19.10	102	80
FPUA5	17.07	103.5	83
FPUA6	16.58	105	84.5

* γ_s: Surface free energy of solid.

The refraction index of the coatings was measured *via* an Abbe refractometer at 25 °C. The obtained refraction indexes for samples PA, FPUA1, FPUA2, FPUA3, FPUA4, FPUA5 and FPUA6 are shown in Fig.3. As we can see, the refraction index value of the samples increases with the introduction of FPU segment. Although fluorine atoms could lead to a relatively low refraction index of materials, the relatively high refraction index of PU structure makes the overall FPUAs maintain at a high refraction index level. This result indicates that the composited FPUA materials could obtain high refraction index and low surface free energy at the same time.

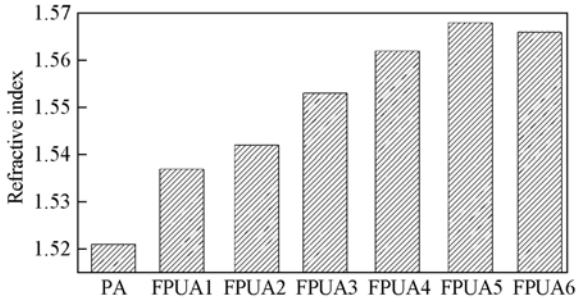

Fig.3 Refraction indexes of the UV-cured coatings

Fig.4 shows the SEM images for the fractured-surface microstructures of FPUAs cured films[Fig.4(A)—(F)] and Fig.5 shows the fractured-surface microstructure of virgin PA. It is observed that the cured pure PA network exhibited very smooth morphology surface, indicating a homogeneous material. However, the fracture surface of fluorine-contained composite FPUA films showed rougher features than that of virgin PA. We can see from SEM micrographs that the phase structures of the inner part of FPUA films are uniform, which showed that PFU and PA were well dispersed to some extent. The micrograph showed that the rough feature only appeared on the top layer of UV-cured FPUA films. These results might be explained as follows: because of the poor compatibility of the fluorinated groups with PA and PU main chain segments, the fluorine-contained groups at the cap of FPU chain segment moved toward the top surface of the coating mixtures during the process of solvent evaporation. The crosslinking reaction was favored under the UV condition between the fluorinated PU and polyacrylate. The coordination of FPU and PA resulted in a continuous phase in their interphase which enhanced the mechanical properties of the composite UV-cured films. The fluorine-contained groups on the top layer could provide a

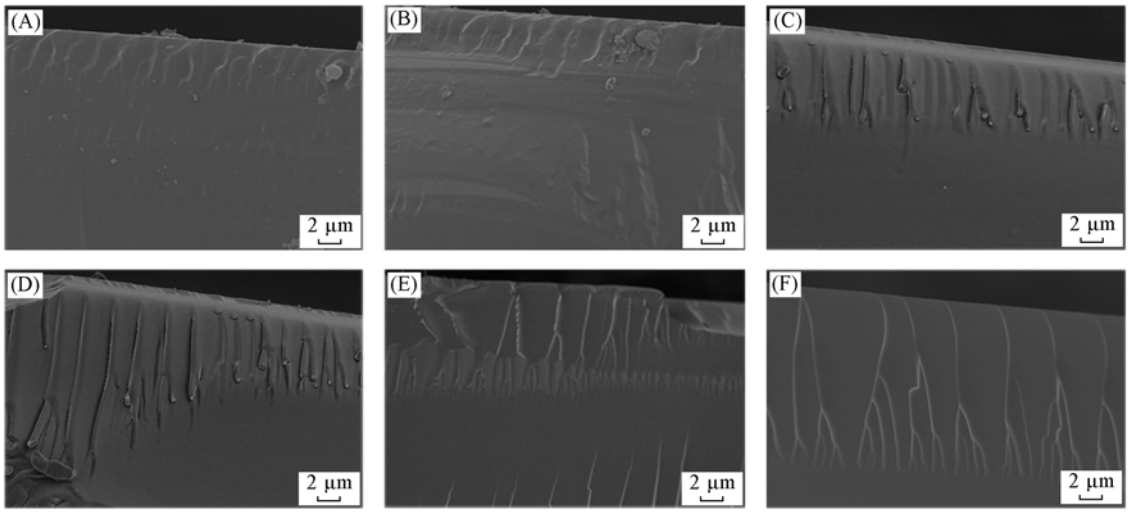

Fig.4 SEM images of fractured-surface microstructures of UV-cured coatings

(A) FPUA1; (B) FPUA2; (C) FPUA3; (D) FPUA4; (E) FPUA5; (F) FPUA6.

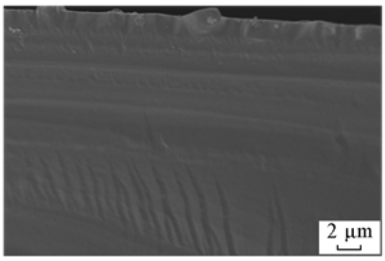

Fig.5 SEM image of fractured-surface microstructure of virgin PA

rather low surface energy, which agrees well with the results of mechanical and contact angle tests.

3.5 Thermal Properties

The effect of fluorinated polyurethane on the thermal stability of PA was investigated by comparing the TGA curves of the fluorine-contained PUA with that of fluorine-free PA film and the results are shown in Fig.6. The degradation rates of the UV-cured films are shown in Fig.7. To get the further information of the degradation behavior of the cured composite coatings, three specific degradation temperatures were recorded: (1) the temperature of the initial 5% mass loss($T_{5\%}$); (2) the temperature of the 50% mass loss($T_{50\%}$); (3) residual mass percent at 600 °C. These degradation data are summarized in Table 4.

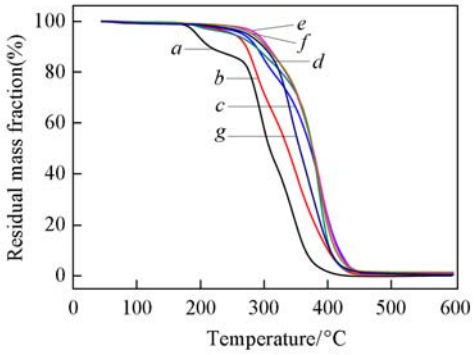

Fig.6 TGA curves of UV-cured coatings

a. PA; *b*. FPUA1; *c*. FPUA2; *d*. FPUA3; *e*. FPUA4; *f*. FPUA5; *g*. FPUA6.

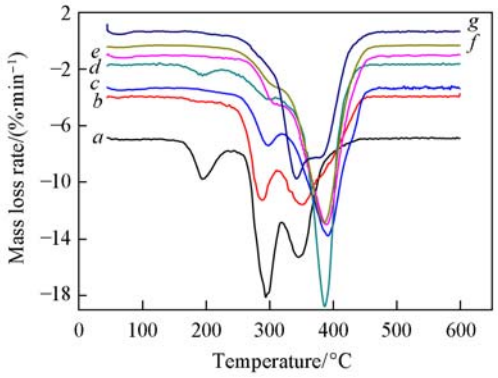

Fig.7 Differential thermal gravity(DTG) curves of the UV-cured coatings

a. PA; *b*. FPUA1; *c*. FPUA2; *d*. FPUA3; *e*. FPUA4; *f*. FPUA5; *g*. FPUA6.

Table 4 Thermal properties of UV-cured coatings

Sample	$T_{5\%}$/°C	$T_{50\%}$/°C	Mass fraction(%) at 600 °C
PA	193.7	308.7	0
FPUA1	249.5	336.7	0.4
FPUA2	252.0	356.5	0.6
FPUA3	266.0	373.5	1.2
FPUA4	282.0	376.0	1.3
FPUA5	288.9	376.7	1.5

It can be seen from Fig.7 that both the fluorine-contained FPUA and the virgin PA exhibit a several-step degradation pattern. According to Fig.7, the first mass loss of PA at around 178 °C is attributed to the dehydration of carboxyl. The second degradation step at around 290 °C corresponds to the depolymerization of the main chain. For fluorine-contained FPUAs, the first degradation step of FPUA1 begins at 290 °C, which is 110 °C higher than that of virgin PA, the second degradation step of FPUA1 begins at around 350 °C. The FPUAs could endure even the temperature reached 350 °C while the PA lost most of its mass. This phenomenon can be explained on the fact that during UV light curing procedure, fluorine-contained segment enriched on the surface of the film, thus, the C—F bond with high bond energy can shield and protect the non-fluorinated inner segment. Thus, the thermal stability of FPUAs is enhanced relative to that of virgin PA, and the delay

in the mass loss of FPUA composites may derive from the barrier effect caused by the steady UV-cured reticular formation and the gather of the fluorine atoms on the surface. As can be seen from Table 4, the 50% mass loss temperature($T_{50\%}$) of FPUA films increased with the increasing of fluorine content. It can be due to well coordination of the fluorinated polyurethane polyacrylate chains with each other in the coating mixtures. Interpenetrating polymer networks caused by UV-radiation make the structure more stable at different temperatures.

4 Conclusions

Novel reactive functional polyacrylate oligomer and fluorine-capped reactive polyurethane were synthesized. A series of UV-curable fluorine-contained FPUAs with different fluorine ratios(1%, 2%, 3%, 4%, 5% and 6%) has been obtained. The structures of the polymers were characterized by FTIR spectrometry. The water absorption, contact angle, SEM, TGA and mechanical tests were performed to check the effect of fluorinated PU on PA. The results show that the water resistance of FPUA is better than that of PA after fluorine was introduced into the system. Contact angle increases with the increase of fluorine content. Besides, it was determined that owing to the hydrophobicity of fluorinated segments, the cured FPUA coating films had low surface free energy. Moreover, the fluorine-contained FPUAs showed an improvement on 5% mass loss temperature, first maximum mass loss temperature and residue amount. SEM micrographs of the cured coatings depict that fluorine-contained groups gathered on the air-side surface of the cured films. It was found from the results that the fluorine plays an important role in the properties such as superficial, mechanical and thermal properties. The low cost hydrophobic UV-curable FPUA coatings have very promising properties which will lead to potential application in advanced industries such as high performance antifouling coatings.

References

[1] Poornima V. P., Jurgen P., Sabu T. J., *Macromol. Sci. A*, **2015**, *52*(5), 353

[2] Koleske J. V., *Radiation Curing of Coatings(No.45)*, *West Conshohocken*, ASTM International, PA, **2002**

[3] Knittel D., Schollmeyer E., *Polym. Intern*., **1998**, *45*, 110

[4] Wang H. L., Liu W. Q., Yan Z. L., Tan J. Q., Xia-Hou G. L., *RSC Adv*., **2015**, *5*, 81838

[5] Pappas S. P., *Radiation Curing: Science and Technology*, Plenum Press, NewYork, **1992**

[6] Lee J. H., Prud'Homme R. K., Aksay I. A., *J. Mater. Res*., **2001**, *16*(12), 3536

[7] Erbay B. T., Serhatli I. E., *Prog. Org. Coat.*, **2013**, *76*(1), 1

[8] Cheng C. J., Zhang X., Huang Q. H., Dou X. Q., Li J., Cao X. X., Tu Y. M., *J. Macromol. Sci. A*, **2015**, *52*(6), 485

[9] Arani Z. K., Ghaffarian S. R., Sadeghi G. M. M., *J. Macromol. Sci. A*, **2014**, *51*(2), 180

[10] Sattar R., Kausar A., Siddiq M., *Chin. J. Polym. Sci*., **2015**, *33*(9), 1313

[11] Xing Q., Li R. B., Dong X., Zhang X. Q., Zhang L. Y., Wang D. J., *Chin. J. Polym. Sci*., **2015**, *33*(9), 1294

[12] Meng X. M., Yang X. H., Wang H. J., Jia R. K., *Chem. Res. Chinese Universities*, **2015**, *31*(4), 680

[13] Xu H., Qiu F., Wang Y., Wu W., Yang D., Guo Q., *Prog. Org. Coat*., **2012**, *73*(1), 47

[14] Li H., Zhang Z. B., Hu C. P., Wu S. S., Ying S. K., *Eur. Polym. J*., **2004**, *40*(9), 2195

[15] Caillier L., de Givenchy E. T., Géribaldi S., Guittard F., *J. Mater. Chem*., **2008**, *18*, 760

[16] Wang X. F., Ni H. G., Xue D. W., Wang X. P., Feng R. R., Wang H. F., *J. Colloid Interface Sci*., **2008**, *321*, 373

[17] Kim Y. S., Lee J. S., Ji Q., McGrath J. E., *Polymer*, **2002**, *43*(25), 7161

[18] Lin Y. H., Liao K. H., Huang C. K., Chou N. K., Wang S. S., Chu S. H., *Polymer International*, **2010**, *59*(9), 1205

[19] Ni H., Gao J., Li X. H., Hu Y. Y., Yan D. H., Ye X. Y., Wang X. P., *J. Colloid Interface Sci*., **2012**, *365*(1), 260

[20] Cui X., Zhong S., Wang H., *Colloids Surf. A*, **2007**, *303*(3), 173

[21] Gao J., Wang X., Wei Y., Yang W., Gao J., Wei Y., *J. Fluorine Chem*., **2006**, 127(2), 282

[22] Wang W., Hua M. Q., Huang Y., Zhang Q., Zhang X. Y., Wu J. B., *Chem. Res. Chinese Universities*, **2015**, *31*(3), 362

[23] Xiong P. T., Lu D. P., Chen P. Z., Huang H. Z., Guan R., *European Polymer Journal*, **2007**, *43*, 2117

[24] Yang J. P., Yuan D. X., Zhou B., Gao J., Ni H. G., Zhang L., Wang X. P., *J. Colloid Interface Sci*., **2011**, *359*(1), 269

[25] Tan H., Xie X. Y., Li J. H., Zhong Y. P., Fu Q., *Polymer*, **2004**, *45*(5), 1495

[26] Honeychuck R. V., Ho T., Wynne K. J., Nissan R. A., *Chem. Mater.*, **1993**, *5*, 1299

[27] *ASTM D2665-84, Standard Specification for Poly(Vinyl Chloride) (PVC) Plastic Drain, Waste, and Vent Pipe and Fittings*, *reapproved*, ASTM International, West Conshohocken, **2009**

[28] *ASTM D522/D522M-13, Standard Test Methods for Mandrel Bend Test of Attached Organic Coatings*, *ASTM International*, West Conshohocken, PA, **2013**.

[29] *ASTM D5963-04(2010)e1, Standard Test Method for Rubber Property-Abrasion Resistance(Rotary Drum Abrader)*, ASTM International, West Conshohocken, **2010**

[30] Owens D. K., Wendt R. C., *J. Appl. Polym. Sci*., **1969**, *13*(8), 1741

[31] Pinnau I., Freeman B. D., *Formation and Modification of Polymeric Membranes: Overview*, Acs Symposium, Washingtaon D. C., **2009**

[32] Çanak T. Ç., Serhatlı İ. E., *Prog. Org. Coat*., **2013**, *76*, 388

[33] Carre A., Malchere A., *J. Colloid Interface Sci*., 1**992**, *149*(2), 379

[34] Girifalco L. A., Good R. J., J. *Phys. Chem*., **1957**, *61*(7), 904

[35] Van Oss C. J., Good R. J., Chaudhury M. K., *Langmuir*, **1988**, *4*(4), 884

[36] Wang Z. G., Appelhans D., Synytska A., Komber H., Simon F., Grundke K., Voit B., *Macromolecules*, **2008**, *41*, 8557